

Automatic Conjunctival Provocation Test Using Hough Transform of Extended Canny Edge Maps

Suman Raj Bista^{1,3}, Serkan Dogan², Anatoli Astvatsatourov², Ralph Mösges², Thomas M. Deserno¹

¹Department of Medical Informatics, RWTH Aachen University, Aachen, Germany

²Department of Medical Statistics, Informatics and Epidemiology, University of Cologne, Cologne Germany

³Centre Universitaire Condorcet, University of Burgundy, Le Creusot, France
sumansrb@gmail.com

Abstract. Computer-aided diagnosis is developed for assessment of allergic rhinitis/rhinoconjunctivitis measuring the relative redness of sclera under application of allergen solution. The patient's eye images are taken from commercial digital camera. The iris is robustly localized using a gradient-based Hough circle transform. From the center of the pupil, the region of interest within the sclera is extracted using geometric anatomy-based a-priori information. The red color pixels are extracted thresholding in the hue, saturation and value color space. Then, redness is measured by taking mean of saturation projected into zero hue. Evaluation is performed with 92 images taken from 13 subjects, 8 responders and 5 non-responders, which were classified according to an experienced otorhinolaryngologist. Provocation is performed with 100, 1,000 and 10,000 AU/ml allergic solution and normalized to control images without provocation. The evaluation yields redness of 1.14, 1.30, 1.60 and 1.04, 1.12, 1.11 for responders and non-responders, respectively. This indicates that our method is suitable as reliable endpoint in controlled clinical trials.

1 Introduction

Atopic diseases such as allergic rhinitis/rhinoconjunctivitis, allergic asthma, and food allergy have increased worldwide [1]. This has been attributed to environmental factors, modulating genetic predisposition, and the natural course of underlying allergic immune responses [2]. Preventive measures and immunomodulatory treatment play an important role in the management of allergic diseases. Therefore, after establishing a tolerated dose range, a dose-response relationship for clinical efficacy must be established. Provocation tests (e.g. conjunctival, nasal or bronchial provocation or allergen exposure in allergen challenge chambers) and/or clinical endpoints may be used as primary endpoints in controlled clinical trials. The conjunctival provocation test (CPT) has been introduced recently to document the course of allergic diseases and the effects of

disease modifying treatments [3]. CPT is performed with grass pollen solutions of three different strengths. However, qualitative inspection of conjunctiva and sclera is highly observer-specific and too subjective as it could be used as a primary endpoint. In this paper, we present a novel method based on automatic processing of color images that is fast, reproducible, accurate, and applicable – at least in principle – to any photographic imaging device.

2 Materials and methods

2.1 CPT protocol

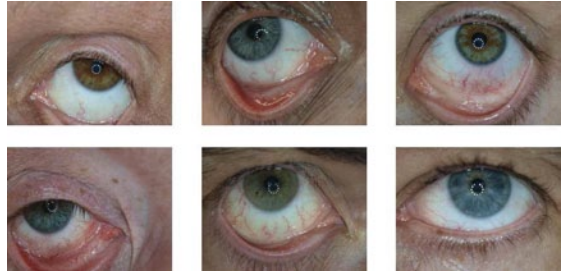
The CPT has been standardized into four consecutive steps.

1. *Preparation*: Firstly, the subject is adapted to the room climate for 10 minutes. Test solutions (expiry date, control temperature, body temperature required) are checked and it is confirmed that the eye is not irritated. Contraindications for CPT (eye diseases except for anomalies of refraction or allergic conjunctivitis, contact lenses, anti-allergic therapy) are excluded. The subject is informed to avoid rubbing his/her eyes during the entire procedure.
2. *Control*: 50 μl of control solution identical to the allergen solution except for allergen content is administered into the lower conjunctival sac of one eye (control eye).
3. *Provocation*: Immediately after application of control solution, administer 50 μl of low-concentrated allergen solution (100 AU/ml) in the lower conjunctival sac of the opposite eye (provocation eye). 10 minutes wait time is taken.
4. *Evaluation*: The response is assessed. If positive, topical antihistamine (e.g. levocabastine, azelastine, emedastine) is administered. If negative, the provocation step is repeated with medium (1,000 AU/ml) and, if again negative, with high concentrated solution (10,000 AU/ml). If it is still negative, CPT is stopped.

2.2 Image acquisition

To derive quantitative measurements, a standard digital SLR (Olympus E3, Japan) with ring light (Hama LED Macro Light, DSLR, Germany) is used to record the eye of the patient. The light is composed of a ring with 12 LEDs for shadow-free illumination of subjects at color temperature of 5500 K. The camera is used with automatic white adjustment disabled. Since the ambient light is dimmed during imaging, the illumination is defined by the LED source. Color calibration patterns are not yet applied, but can be integrated in the process easily. Fig. 1 shows some examples of images. Variations in pupil positioning, focus and blur must be taken into account when designing robust segmentation.

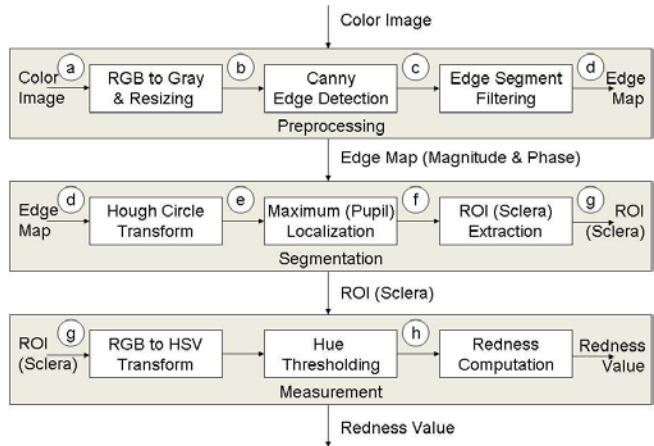
Fig. 1. Images acquired for CPT.



2.3 Image processing

Roughly 20 years ago, the circular Hough transform has been applied robustly by one of the authors for iris localization measuring the angle of squint [4]. Since then, it has been broadly applied in eye pattern analysis and biomedical authentication. Therefore, we rely on a Hough-based strategy for segmentation. The scheme for computer-aided diagnoses (CAD) is illustrated in Fig. 2 and corresponding images are depicted in Fig. 3. At a large scale, we apply pre-processing, segmentation and measurement. All steps have been implemented in Java and plugged into ImageJ.

Fig. 2. Image processing chain.



Pre-processing aims at normalization and speeding up the segmentation procedure. After color to 8 bit gray transform, the images are reduced from 3648 x 2736 pixels (Fig. 3a) down to 256 x 192 pixel (Fig. 3b) using linear interpolation [5]. A modified Canny edge detection approach is used to extract prominent edges, where – in addition to the original Canny algorithm – the direction of gradient is captured in a separate phase map [4]. The magnitude is then thresholded according to the hysteresis approach introduced by Canny, and a binary edge image is obtained (Fig. 3c). Applying connected components analysis, short

ments are removed automatically (Fig. 3d). A minimum segment length of pixels is applied, but this threshold is not critical. Segmentation aims at automatic extraction of the sclera ROI. As derived from Fig. 1, the iris forms a prominent circle that is usable as landmark. The center of the iris corresponds to the center of the pupil and is detected using a directive circular Hough transform [4]. Fig. 3e illustrates the resulting three-dimensional accumulator array, which has been sliced at the corresponding radius r . The peak in the Hough space is clearly indicated even if the iris is partly covered by the eyelid. After peak localization, center and radius are projected back to the original scale. Fig. 3f illustrates two circles, $(r + \alpha)$ and $(\beta \cdot r)$, where the thresholds α and β have been determined heuristically as global constant from known geometry of fully grown human eyes.

According to the pupil positioning, two angles α_l and α_r for left and right eye, respectively, are used to extract the final ROI, which is completely positioned within the sclera and the parameters α , β , and γ are selected such that the area of the ROI is maximized (Fig. 3g). Measurement aims at quantitatively

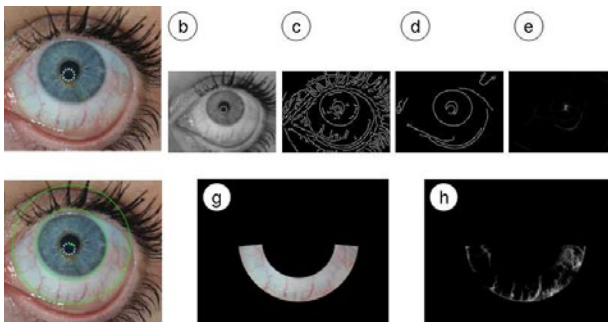


Fig. 3. Results according to image processing chain of Fig. 2.

determine the redness of the sclera, since the blood vessels expand in response to the provocation. Red, green and blue (RGB) color space is converted into the hue, saturation, value (HSV) space, which better corresponds to semantic color concepts. Disregarding the value (indication of brightness), color is represented as a disc of radius S . A symmetric section around H_0 is extracted, where H_0 represents the color red. In addition, all pixels with low saturation are excluded from further evaluation (Fig. 4). The resulting amount of red pixels is visualized in Fig. 3h. The redness R is measured by taking mean of saturation projected

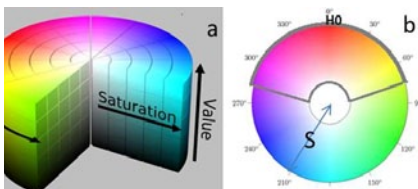


Fig. 4. Thresholding in HSV color space.

into zero hue according to 1, where N denotes the total number of red pixels after thresholding

$$R = \frac{1}{N} \sum_{n=0}^{N-1} (S_n \cdot \cos H_n) \quad (1)$$

2.4 Evaluation study

In a first evaluation study, 13 patients have been applied to 50 μl of 100, 1000, and 10,000 AU/ml concentrated allergen solution, consecutively. Visual inspection by an otorhinolaryngologist categorizes the subjects into two groups, responder vs. non-responder, and 8 vs. 5 subjects resulted for each of the classes, respectively. N repeated measurements were made at each step (Tab. 1). In total, 92 images have been acquired. Mean and standard deviation of redness for responders and non-responders were computed according to (1) and normalized to the control image (Step 2 of CPT protocol).

3 Results

Fig. 3 illustrates the step-wise processing of images. All photographs were processed successfully. The Hough transform and iris center as well as radius detection performed errorless and accurate for all images disregarding partial occlusion, blur, and noise. This indicates the robustness of image processing. For the group of responders, the relative redness is measured as 1.14, 1.30, and 1.60 for 100, 1000 and 10,000 AU/ml respectively. The group of non-responders yields 1.04, 1.12, and 1.11, respectively (Tab. 1).

4 Discussion

A simple and robust image processing chain has been developed that quantifies CPT making it applicable as primary end point in controlled clinical trials and for quantitative assessment of allergic diseases. Accordingly, a pilot study is planned with 100 subjects using this measure.

So far, we do not apply color pattern and color calibration. This is likely to lower the standard deviation of the redness measure and enable also absolute color assessment. Also, the parameters α , β , and γ will be determined automatically in future. This can be done adding some heuristics into the chain of image processing. Then, the entire process becomes fully automatic.

However, our small evaluation study has already shown that the relative redness is increased significantly for the group of responders, whilst a rather constant redness is obtained for those subjects that have been rated as non-responder. The outlier in Table 1a (subject 2118) is due to incomplete opening of the eye, where the important area is covered by the lower eyelid (Fig. 1, bottom right). In summary, we conclude that the proposed image processing chain is suitable for computer-aided diagnosis in allergic rhinitis/rhinoconjunctivitis.

Table 1. Redness measurement. Dose: a = 0, b = 100, c = 1,000, d = 10,000 AU/ml.

Responders				Non-responders							
ID	Dose	<i>N</i>	<i>R</i>	ID	Dose	<i>N</i>	<i>R</i>				
A	a	1	1.000	E	a	2	1.000	I	a	1	1.000
	b	2	1.364		b	1	1.242		b	2	1.364
	c	2	1.440		c	1	1.254		c	2	1.440
	d	3	1.494		d	1	1.330		d	3	1.494
B	a	1	1.000	F	a	1	1.000	J	a	1	1.000
	b	1	1.023		b	1	1.065		b	2	1.079
	c	3	1.037		c	2	1.083		c	2	1.199
	d	3	2.018		d	2	1.091		d	2	1.078
C	a	1	1.000	G	a	1	1.000	K	a	1	1.000
	b	4	1.134		b	3	1.243		b	1	1.070
	c	2	1.240		c	2	1.666		c	1	1.001
	d	5	1.423		d	2	1.988		d	2	0.937
D	a	1	1.000	H	a	1	1.000	L	a	1	1.000
	b	2	1.548		b	1	0.525		b	2	1.089
	c	2	1.648		c	2	1.034		c	2	1.140
	d	2	2.139		d	2	1.334		d	2	2.171
Total					a	9	1 ± 0		a	5	1 ± 0
					b	15	1.143 ± 0.30		b	8	1.108 ± 0.16
					c	16	1.299 ± 0.26		c	9	1.161 ± 0.18
					d	20	1.602 ± 0.39		d	10	1.147 ± 0.21

References

1. Ait-Khaled N, Pearce N, Anderson H, et al. Global map of the prevalence of symptoms of rhinoconjunctivitis in children—the international study of asthma and allergies in childhood (ISAAC) Phase Three. *Allergy*. 2009;64(1):122–48.
2. Mösges R, Klimek L. Today's allergic rhinitis patients are different: new factors that may play a role. *Allergy*. 2007;62(9):969–75.
3. Riechelmann H, Epple B, Gropper G. Comparison of conjunctival and nasal provocation test in allergic rhinitis to house dust mite. *Int Arch Allergy Immunol*. 2003;130(1):51–9.
4. Kaupp A, Lehmann T, Effert R, et al. Automatic measurement of the angle of squint by Hough-transformation and covariance-filtering. *Proc IAPR Int Conf Pattern Recogn*. 1994;1:784–6.
5. Lehmann TM, Gönner C, Spitzer K. Addendum: B-spline interpolation in medical image processing. *IEEE Trans Med Imaging*. 2001;20(7):660–5.